Published in final edited form as:
Diabetologia. 2011 April ; 54(4): 935–944. doi:10.1007/s00125-010-1984-5.

Knockdown of the gene encoding Drosophila tribbles homologue 3 (*Trib3*) improves insulin sensitivity through peroxisome proliferator-activated receptor-γ (PPAR)-γ activation in a rat model of insulin resistance

D. Weismann[1,6], **D. M. Erion**[1,2,3], **I. Ignatova-Todorava**[1], **Y. Nagai**[1], **R. Stark**[1], **J. J. Hsiao**[1], **C. Flannery**[1], **A. L. Birkenfeld**[1], **T. May**[3], **M. Kahn**[3], **D. Zhang**[3], **X. X. Yu**[5], **S. F. Murray**[5], **S. Bhanot**[5], **B. P. Monia**[5], **G. W. Cline**[1], **G. I. Shulman**[1,2,3], and **V. T. Samuel**[1,4]

[1]Section of Endocrinology, Department of Internal Medicine PO BOX 802010, Yale University School of Medicine, New Haven, CT 06520-8020, USA

[2]Department of Cellular and Molecular Physiology, Yale University School of Medicine, New Haven, CT, USA

[3]Howard Hughes Medical Institute, Yale University School of Medicine, New Haven, CT, USA

[4]Veterans Affairs Medical Center, West Haven, CT, USA

[5]Isis Pharmaceuticals, Carlsbad, CA, USA

[6]Universitätsklinikum Würzburg, Medizinische Klinik und Poliklinik I, Schwerpunkt Endokrinologie und Diabetologie, Würzburg, Germany

Abstract

Aims/hypothesis—Insulin action is purportedly modulated by Drosophila tribbles homologue 3 (TRIB3), which in vitro prevents thymoma viral proto-oncogene (AKT) and peroxisome proliferator-activated receptor (PPAR)-γ activation. However, the physiological impact of TRIB3 action in vivo remains controversial.

Methods—We investigated the role of TRIB3 in rats treated with either a control or *Trib3* antisense oligonucleotide (ASO). Tissue-specific insulin sensitivity was assessed in vivo using a euglycaemic–hyperinsulinaemic clamp. A separate group was treated with the PPAR-γ antagonist, bisphenol-A-diglycidyl ether (BADGE) to assess the role of PPAR-γ in mediating the response to *Trib3* ASO.

Results—*Trib3* ASO treatment specifically reduced *Trib3* expression by 70 to 80% in liver and white adipose tissue. Fasting plasma glucose, insulin concentrations and basal rate of endogenous glucose production were unchanged. However, *Trib3* ASO increased insulin-stimulated whole-body glucose uptake by ~50% during the euglycaemic–hyperinsulinaemic clamp. This was

Address correspondence to: V. T. Samuel, varman.samuel@yale.edu.

Duality of interest

X. X. Yu, S. F. Murray, S. Bhanot and B. P. Monia own stock and/or hold stock options in Isis Pharmaceuticals. All other authors declare that there is no duality of interest associated with this manuscript.

attributable to improved skeletal muscle glucose uptake. Despite the reduction of *Trib3* expression, AKT2 activity was not increased. *Trib3* ASO increased white adipose tissue mass by 70%, and expression of *Ppar*-γ and its key target genes, raising the possibility that *Trib3* ASO improves insulin sensitivity primarily in a PPAR-γ-dependent manner. Co-treatment with BADGE blunted the expansion of white adipose tissue and abrogated the insulin-sensitising effects of *Trib3* ASO. Finally, *Trib3* ASO also increased plasma HDL-cholesterol, a change that persisted with BADGE co-treatment.

Conclusions/interpretation—These data suggest that TRIB3 inhibition improves insulin sensitivity in vivo primarily in a PPAR-γ-dependent manner and without any change in AKT2 activity.

Keywords

Antisense oligonucleotide; Euglycaemic–hyperinsulinaemic clamp; Insulin sensitivity; PPAR gamma; TRIB3

Introduction

Insulin signalling in muscle and liver share common pathways that converge on key kinases, such as serine/threnonine kinase AKT2. In liver, insulin-mediated AKT2 activation regulates hepatic glucose production by promoting glycogen synthesis and inhibiting gluconeogenesis [1]. AKT2 activation is an essential step for insulin-induced GLUT4 translocation in skeletal muscle, promoting glucose uptake [1–3]. In the pathogenesis of insulin resistance, accumulation of diacylglycerol in muscle and liver leads to activation of novel protein kinase Cs (θ and ε, respectively) that inhibit insulin signalling and impair activation of AKT2 [1, 4, 5]. However, cells also possess inherent mechanisms to negatively regulate insulin signalling. Recently, the Drosophila tribbles homologue 3 (TRIB3) was identified as a negative regulator of AKT activity in human embryonic kidney 293 cells and mouse liver [6]. Fasting induces hepatic TRIB3 production and TRIB3 is highly upregulated in diabetic *db/db* mice [7]. TRIB3 production is also increased in other experimental conditions associated with insulin resistance, such as high-fructose feeding [8] or chronic ethanol consumption [9]. Insulin may also cause increased TRIB3 production, suggesting a possible pathway whereby hyperinsulinaemia could lead to impaired insulin signalling [10].

TRIB3 has been implicated in insulin resistance in humans. Liu et al. reported that TRIB3 protein levels are significantly elevated in patients with type 2 diabetes mellitus [11]. In that cohort, higher levels of TRIB3 protein were associated with hyperglycaemia and reduced insulin-stimulated whole-body glucose disposal, suggesting that TRIB3 content was closely associated with the development of insulin resistance [11]. Aside from changes in abundance, polymorphisms that affect the function of TRIB3 have also been implicated in the development of insulin resistance and type 2 diabetes mellitus in humans. Specifically, the Q84R missense polymorphism has been associated with worsening insulin resistance and dyslipidaemia [12, 13]. Prudente et al. found an association between this polymorphism and some features of the metabolic syndrome [12]. In a larger analysis, they also reported an association between the R84 polymorphism and an increased risk of type 2 diabetes mellitus, especially among individuals who are 45 years of age or younger [14]. Andrezzoni

et al. suggest that this polymorphism may also lead to endothelial dysfunction [15]. Using human umbilical embryonic vein endothelial cells isolated from individuals who were either heterozygous or homozygous for the R84 (i.e. QR or RR) polymorphism, they demonstrated that the R84 polymorphism impaired insulin-mediated increases in endothelial nitric oxide synthase activity. This substitution of arginine for glutamine at position 84 is thought to enhance the ability of TRIB3 to impede AKT2 activation [12] possibly by enhancing the binding between TRIB3 and AKT2 [15]. Together, these studies suggest that increases in TRIB3 activity are closely associated with insulin resistance and type 2 diabetes mellitus, primarily via inhibition of AKT2 activation.

However, this conclusion is still controversial. Iynedjian reported that overproduction of TRIB3 in hepatocytes had no effect on insulin signalling [16] and Okamoto et al. report that deletion of *Trib3* in mice did not alter insulin-stimulated glucose metabolism [17]. Moreover, TRIB3 has been implicated in the regulation of other proteins. In beta cells, TRIB3 may bind with activating transcription factor 4 (ATF4) to inhibit cAMP responsive element binding protein 1 (CREB1)-mediated production of proteins critical to exocytosis of insulin-containing granules (potentially accounting for the decrease in insulin secretion seen in humans with the Q84R polymorphism) [14, 18]. In adipocytes, Trib3 has been reported to interact with peroxisome proliferator-activated receptor (PPAR)-γ in vitro. TRIB3 suppresses adipocyte differentiation by negatively regulating PPAR-γ transcriptional activity, while knockdown of TRIB3 in 3T3-L1 cells promotes adipocyte differentiation [19].

Here, we sought to clarify the physiological role of TRIB3 and investigate its potential as a therapeutic target in a rat model of type 2 diabetes mellitus, in which *Trib3* was knocked down with antisense oligonucleotides (ASO). Following treatment, changes in liver, muscle and adipose insulin action were assessed by euglycaemic–hyperinsulinaemic clamps in awake rats.

Methods

Animals

All procedures were approved by the Institutional Animal Care and Use Committee of the Yale University School of Medicine. Male Sprague–Dawley rats (150 g) were received from Charles River Laboratories (Wilmington, MA, USA) and given 3 days to acclimatise. Rats were then given a 100 mg/kg dose of nicotinamide by intraperitoneal injection and 15 min later received a 65 mg/kg dose of streptozotocin. Rats had a 4 day recovery period prior to the first ASO injection. Rats were housed individually on a 12 h light–dark cycle, with free access to food and water. Body weight and food consumption were monitored weekly. Animals were fed a high-fat diet (energy intake 26% carbohydrate, 59% fat, 15% protein), in which the major constituent is safflower oil. While on high-fat diet, rats were treated with ASO (75 mg/kg per week, given twice weekly i.p.). This model has previously been shown to prevent the hyperinsulinaemia seen with high-fat feeding alone [20] and has also been associated with muscle and liver insulin resistance [21].

Selection of rat Trib3 ASO

To identify rat *Trib3* ASOs, rapid-throughput screens were performed in vitro as previously described [22]. In brief, 80 ASOs were designed to the *Trib3* mRNA sequence. Initial screens identified several potent and specific ASOs, all of which targeted a binding site within the coding region of *Trib3* mRNA. After extensive dose–response characterisation, the most potent ASO from the screen was chosen. It was ISIS-391274, and had the following sequence: 5′-GTCCAGTCATCACACAGGCA-3′. The control ASO, ISIS-141923, has the sequence 5′-CCTTCCCTGAAGGTTCCTCC-3′ and does not have perfect complementarity to any known gene in public databases. The first five bases and last five bases of chimeric ASOs have a 2′-*O*-(2-methoxy)-ethyl modification; the ASOs also have a phosphorothioate backbone. This chimeric design has been shown to provide increased nuclease resistance and mRNA affinity, while maintaining the robust RNase H terminating mechanism used by these types of ASOs [23]. These benefits result in an attractive in vivo pharmacological and toxicological profile for 2′-*O*-(2-methoxy)-ethyl chimeric ASOs.

Co-administration of the PPAR-γ antagonist bisphenol-A-diglycidyl ether

Rats had unrestricted access to a 27% (wt/wt) high-fat diet and were treated with *Trib3* or control ASO as described above. For the last 8 days of ASO treatment, the PPAR-γ antagonist bisphenol-A-diglycidyl ether (BADGE) (Cayman Chemical, Ann Arbor, MI, USA) was subcutaneously injected once daily (1 mg/kg body weight) [24].

Euglycaemic–hyperinsulinaemic clamp studies

Some 7 to 9 days prior to the euglycaemic–hyperinsulinaemic clamp, catheters were inserted into the right internal jugular vein extending to the right atrium and the left carotid artery extending into the aortic arch. Subsequently the rats were fasted overnight (from 18.00 hours) and on the following morning (06.00 hours) were infused with [6,6-2H]glucose (99% enriched, 6.1 nmol/kg prime, 0.5 nmol/kg) infusion to assess basal glucose turnover. After the basal period, the euglycaemic–hyperinsulaemic clamp was conducted for 140 min with a primed/continuous infusion of insulin (400 mU/kg prime over 5 min, thereafter 4 mU/kg per min) and a variable infusion of 20% (wt./vol.) dextrose enriched with 2.5% [6,6-2H]glucose to maintain euglycaemia. At 0 and 140 min additional blood was drawn to determine various blood proteins and metabolites. Upon completion of the clamp, rats were anaesthetised with pentobarbital sodium injection (150 mg/kg) and all tissues were extracted and frozen immediately using liquid N_2-cooled aluminium tongs. Tissues were stored at −80° C for subsequent analysis.

Liver insulin signalling

A separate group of rats that were treated exactly the same as the previous were used to investigate the effect of TRIB3 treatment on insulin signalling. These rats underwent a 20 min euglycaemic–hyperinsulinaemic clamp. Immediately after the clamp, rats were killed and the liver removed and subsequently frozen using liquid N_2-cooled brass tongs. The activity of AKT was assessed by measuring the incorporation of ^{32}P into a synthetic AKT substrate as previously described [25].

Biochemical analysis and calculations

Plasma glucose was determined during the clamp using 10 µl plasma and the glucose oxidase method performed by an analyser (Beckman Glucose Analyzer II; Beckman Coulter, Brea, CA, USA). Plasma insulin, glucagon, leptin and adiponectin concentrations were determined using an assay system (Lincoplex; Linco Research, St Charles, MO, USA). For fast protein liquid chromatography (FPLC) analysis, samples from control ASO and *Trib3* ASO were pooled, injected on to an AKTa FPLC (Amersham Pharmacia Biotech, Piscatawy, NJ, USA) and eluted at a constant flow rate of 0.5 ml/min FPLC buffer (0.15 mol/l NaCl, 0.01 mol/l Na2HPO4, 0.1 mmol/l EDTA, pH 7.5). To determine the enrichment of plasma glucose, 30 µl of the designated samples were deproteinised in 150 µl 100% methanol. The samples were dried overnight and derivatised with 1:2 acetic anhydride:pyridine to produce the pentacetate derivative of glucose. The atom percentage enrichment of 6,6-2H glucose was then measured by gas chromatographic/mass spectrometric analysis using a gas chromatograph (Hewlett-Packard 5890; GMI, Ramsey, MN, USA) interfaced to a mass-selective detector (Hewlett-Packard 5971A) operating in the electron ionisation mode [26]. The atom per cent excess of glucose m+2 was determined from the m:z ratio 202:200.

Tissue lipid measurement

The purification of diacylglycerol from liver was performed as previously described [27, 28]. After purification, fatty acyl-CoA fractions were dissolved in methanol:H_2O (1:1, vol./vol.) and subjected to liquid chromatography/mass spectrometry/mass spectrometry analysis. A turbo ion spray source was interfaced with a tandem mass spectrometer (API 3000; Applied Biosystems, Carlsbad, CA, USA) in conjunction with two micro pumps and an autosampler (200 Series; PerkinElmer, Waltham, MA, USA). Total diacylglycerol content is expressed as the sum of individual species. Triacylglycerol was extracted using the method of Bligh and Dyer [29] and measured with a commercially available kit (DCL Triglyceride Reagent; Diagnostic Chemicals, Oxford, CT, USA).

Total RNA preparation and real-time quantitative RT-PCR analysis

Total RNA was extracted from liver samples using a kit (RNeasy; Qiagen, Valencia, CA, USA). RNA was reverse-transcribed into cDNA with reverse transcriptase (StrataScript; Stratagene, Santa Clara, CA, USA). The abundance of transcripts was assessed by real-time PCR (7500 Fast Real-Time PCR System; Applied Biosystems) with SYBR Green detection system (Stratagene). For each run, samples were run in duplicate for the gene of interest and β-actin. The expression data for each gene of interest and β-actin were normalised for the efficiency of amplification, as determined by a standard curve included on each run [30].

Immunoblots

White adipose tissue, liver and muscle specimen were ground with a mortar and pestle, mixed with 1 ml of lysis buffer (50 mmol/l Tris-HCl buffer [pH 7.5 at 4 °C], 50 mmol/l NaF, 5 mmol/l NaPPi, 1 mmol/l EDTA, 1 mmol/l EGTA, 1 mmol/l dithiothreitol, 1 mmol/l benzamidine, 1 mmol/l phenylmethanesulfonyl fluoride, glycerol [10% vol./vol.], Triton X-100 [1% vol./vol.], 1 µmol/l trichostatin A and 50 mmol/l nicotinamide) and homogenised

for 30 s. Homogenates were spun at 20,800 *g* for 10 min at 4 °C and protein concentrations were determined. SDS gel electrophoresis was performed using precast Bis-Tris 4 to 12% gradient polyacrylamide gels in the Mops buffer system (Invitrogen, CA, USA). After transfer to nitrocellulose membranes, membranes were incubated in blocking buffer (5% [wt/vol.] milk) for 1 h and immunoblotted with TRIB3 (Santa Cruz, Heidelberg, Germany), β-actin (Santa Cruz), phospho-AKT (Cell Signaling Technology, MA, USA) and AKT (Cell Signaling Technology) antibodies. After incubation with the primary antibody, the membranes were washed three times for 15 min with Tris-buffered saline (10 mmol/l Tris-HCl [pH 7.4], 0.5 mol/l NaCl) plus Tween 20 (0.2% vol./vol.) (TBST). The membranes were immersed in blocking buffer and a corresponding IgG-conjugated secondary antibody, and incubated for 2 h. The membranes were then washed three times for 5 min using TBST. Proteins were then detected with enhanced chemiluminescence (Thermo Fisher Scientific, Waltham, MA, USA) and autoradiographs were quantified by densitometry (ImageJ).

Statistical analysis

All values are expressed as the mean ± SEM. The significance between the mean values was evaluated by two-tailed unpaired Student's *t* test. Significance is indicated as $*p<0.05$, $**p<0.01$ and $***p<0.001$. Statistical analysis was performed with the statistical software R [31].

Results

Trib3 ASO is specific and effective

Trib3 ASO treatment specifically reduced *Trib3* expression in liver (by 70%) and epididymal white adipose tissue (by 80%) after 4 weeks of treatment at 75 mg/kg per week. No significant differences were seen for *Trib1* and *Trib2* expression in liver or white adipose tissue (Fig. 1a–d). Body weight and food intake were similar in both groups. No differences were seen in fasting plasma glucose, insulin and glucagon levels, or in alanine transferase and aspartate transferase plasma concentrations (Table 1). Surprisingly, epididymal white adipose tissue mass increased by 70% following *Trib*3 ASO treatment (Table 1). This was associated with a 25% increase in plasma adiponectin concentrations, but without any differences in plasma leptin concentration (Table 1).

Trib3 ASO increases peripheral insulin sensitivity

We quantified the effects of reduced *Trib3* expression on hepatic and peripheral insulin sensitivity using euglycaemic–hyperinsulinaemic clamps in awake, unrestrained rats (n=12 per group) [4]. *Trib3* ASO did not affect rates of endogenous glucose production either under basal or euglycaemic–hyperinsulinaemic conditions (Fig. 2a, c). However, under euglycaemic–hyperinsulinaemic conditions, *Trib3* ASO did increase the rate of whole-body glucose uptake by 47% (Fig. 2d). This increase in insulin-stimulated peripheral glucose disposal was largely accounted for by improved skeletal muscle glucose uptake. Peripheral 2-deoxy[^{14}C]glucose uptake was 30% and 40% higher in tibialis anterior and soleus muscle (Fig. 3b, g). Although 2-deoxy[^{14}C]glucose uptake in epididymal white adipose tissue, assessed on a per gram basis, was not significantly altered with *Trib3* ASO (1.1±0.12 vs 0.87±0.13, NS; see Electronic supplementary material [ESM] Fig. 1 a, b), the increased

adipose tissue mass also contributes to the increase in whole-body insulin-stimulated glucose uptake. In addition, *Trib3* ASO modestly enhanced the ability of insulin to suppress plasma NEFA concentration (Table 1).

Trib3 ASO increases PPAR-γ activity in epididymal white adipose tissue

To determine the cause of increased adipose tissue mass, we measured levels of *Ppar*-γ and downstream targets. PPAR-γ levels were increased by 87% in the white adipose tissue of *Trib3* ASO treated animals. Consistent with increased PPAR-γ activity, the expression of downstream genes such as CCAAT/enhancer binding protein alpha (*Cebpa*), *Cd36* and acyl-CoA oxidase [19, 24] was also increased (Fig. 1e). To assess the specific role of PPAR-γ activation following *Trib3* ASO treatment, an additional set of animals was treated with the PPAR-γ antagonist BADGE for the last 8 days of ASO administration [24]. Again, *Trib3* ASO significantly decreased *Trib3* levels in liver and white adipose tissue. Body weight and food intake remained similar in animals treated with BADGE + *Trib3* ASO and BADGE + control ASO. However, BADGE co-treatment prevented the increased expression of *Ppar*-γ and of its downstream targets, *Cebpa*, *Cd36* and acyl-CoA oxidase (Fig. 1f). Moreover, in contrast to *Trib3* ASO treatment alone, co-treatment with BADGE prevented the expansion of adipose tissue (Table 1). The increased insulin sensitivity during euglycaemic–hyperinsulinaemic portion of the clamp was also completely abolished after BADGE treatment, with no differences in whole-body glucose disposal or hepatic glucose production (Fig. 2b–d).

Trib3 ASO increases HDL-cholesterol

Although plasma triacylglycerol and fatty acid concentrations were similar in both groups, we observed a 40% increase in plasma total cholesterol concentration in *Trib3* ASO-treated animals (Table 1). This increase was accounted for by a 50% increase of the HDL fraction, as confirmed by FPLC-based size separation of lipoproteins. The increase in plasma HDL-cholesterol was associated with increased levels of sterol regulatory element binding factor 2 (*Srebp2*) but without any change in scavenger receptor class B, member 1 (*Sr-b1* [also known as *Scarb1*]) or ATP-binding cassette, sub-family A, member 1 (*Abca1*). Importantly, increased HDL levels were also observed after BADGE treatment, indicating that these effects were independent of PPAR-γ activation (Table 1).

Insulin signalling

TRIB3 has been shown to inhibit activation of AKT and by extension insulin signalling in vitro. Thus, we hypothesised that knockdown of *Trib3* would increase AKT2 activity and enhance hepatic insulin action. However, there was no difference in hepatic AKT2 activity in the basal state, or after 20 min or 120 min of insulin stimulation (end of clamp) (Fig. 4a). Similarly, *Trib3* ASO did not alter white adipose tissue AKT phosphorylation and AKT activity despite a significant knockdown of *Trib3* (Fig. 4e, ESM Fig. 1a). We also assessed AKT2 activation by assessing site-specific phosphorylation. There was no difference in AKT phosphorylation on the Thr 308 residue in liver, adipose tissue and muscle after insulin stimulation, and no difference in phosphorylation of Ser 473 residue in liver and white adipose tissue (ESM Fig. 2a, b).

Interestingly, although ASOs do not directly decrease target expression in skeletal muscle, we found a trend towards reduced *Trib3* expression in the soleus (40% reduction compared with control ASO, p=0.09) (Fig. 3a). This was accompanied by a significantly higher glucose uptake in the soleus (Fig. 3b). Unlike in liver or white adipose tissue, these changes in *Trib3* expression were abolished by BADGE treatment (Fig. 3a). This may be a secondary effect related to improved insulin sensitivity, as insulin itself has been shown to modulate *Trib3* expression in vitro [32]. The increases in whole-body insulin-mediated glucose disposal developed without increase of insulin-stimulated AKT2 activity (Fig. 3d). Again, we confirmed the results of the AKT2 activity assay by examining AKT2 phosphorylation. In the soleus, although there were no differences in phosphorylation at Thr 308, there was a mild decrease in Ser 473 phosphorylaton (ESM Fig. 2c). The increase in plasma adiponectin may also improve insulin action via activation of AMP-activated protein kinase (AMPK) [33]. Despite elevated adiponectin levels, we did not detect a significant increase in AMPK-activity in soleus (Fig. 3c).

Discussion

Insulin regulates diverse metabolic pathways within the cell via intricate networks of signalling proteins. These networks converge on key focal points, one of which is activation of AKT2 [3]. Recently TRIB3, the mammalian homologue of the Drosophila tribbles, has been identified as a negative regulator of AKT2. Its abundance is increased in rodent models of type 2 diabetes mellitus, as well as with fasting. In both cases, this is associated with decreased AKT2 activation [6, 8–10, 34, 35]. In addition, production of TRIB3 itself may also be induced by insulin and may be the effector of a negative feedback loop [10, 32]. In vitro studies have demonstrated that TRIB3 inhibited AKT2 in HepG2 cells and that adenoviral-mediated increases in hepatic *Trib3* expression in normal mice impaired glucose disposal [6]. However, genetic deletion of *Trib3* in mice failed to alter glucose metabolism or AKT activation following insulin stimulation [17], casting doubt on the physiological relationship between TRIB3 and AKT. In addition, TRIB3 has been shown to partner with other proteins, notably PPAR-γ and CEBPB [32]. We sought to understand the physiological role of TRIB3 in vivo, as a potential regulator of insulin action and glucose metabolism, using specific ASOs to knockdown *Trib3* in rats. Accordingly, we hypothesised that knockdown of *Trib3* would enhance AKT2 activation and improve hepatic insulin sensitivity in a rat model of insulin resistance.

Although ASO treatment effectively and selectively reduced hepatic *Trib3* expression by 70%, there was, surprisingly, no effect on basal and insulin-mediated activation of AKT2 in the liver, either at 20 min following insulin stimulation or at the end of a 120 min euglycaemic–hyperinsulinaemic clamp. Consistent with this, no difference was observed in hepatic insulin sensitivity. In white adipose tissue, *Trib3* expression was similarly decreased, but, again, no differences were observed in glucose uptake or in the degree of AKT phosphorylation in the basal state or after insulin stimulation (Fig. 4e). Furthermore, analysis of the phosphorylation state of the Thr 308 residue, which is essential for AKT activation [36], and of the Ser 473 residue, which is required for maximal stimulation of AKT, revealed no difference in liver and white adipose tissue. Consistent with this observation, AKT2 activation was not altered in *Trib3*$^{-/-}$ mice studied under normal chow conditions

[17]. Thus, while it remains possible that *Trib3* overexpression may inhibit AKT2 activation, the inverse may not be true. Specifically, inhibition of TRIB3 does not enhance AKT2 activity. Instead, we propose, that the improvements in insulin action following knockdown of *Trib3* are primarily a function of augmented PPAR-γ activity in the adipose tissues.

The transcriptional control of adipogenesis requires careful orchestration of multiple regulatory proteins. Early adipogenesis is characterised by increased abundance of Cebpb and Cepbd. These proteins are thought to set the stage for the later stages of adipogenesis, which require the increased levels of CEBPA and PPAR-γ [37]. These proteins increase each other's production and bind to a remarkably similar number of target genes [38]. Previous in vitro studies in 3T3-L1 pre-adipocytes demonstrated a role for TRIB3 in adipogenesis [19, 39]. Overproduction of TRIB3 in 3T3-L1 cells may impair the early steps of adipogenesis. Here, TRIB3 is thought to inhibit CEBPB transcription by preventing its phosphorylation by extracellular signal-regulated kinases 1 and 2, as well as by directly interfering with its ability to bind DNA. This, in turn, inhibits its ability to increase production of PPAR-γ2. Takahashi et al. explored the role of TRIB3 late in the differentiation of 3T3-L1 cells [19]. They report that TRIB3 directly binds to and inhibits PPAR-γ in 3T3-L1 pre-adipocytes, leading to decreased production of PPAR-γ and CEBPA, and key target genes, and ultimately impairing adipocyte differentiation. In those studies, CEBPB production was not altered at any time point. Thus, it is possible that TRIB3 may have different inhibitory roles throughout adipogenesis. In the early stages, it may impair CEBPB activity and in the later stages PPAR-γ.

In the present study we found that ASO-mediated decrease of *Trib3* augmented PPAR-γ activity in vivo, leading to improvements in insulin sensitivity, increased fat mass and increased expression of genes downstream of PPAR-γ such as acyl-CoA oxidase, *Cd36* and *Cebp*α. We found that increased PPAR-γ activity was associated with increased *Ppar*-γ expression. It is likely that this represents a feed-forward activation of PPAR-γ by itself, which has previously been shown to be dependent on increased levels of CEBPA [40]. Although insulin-stimulated white adipose tissue 2-deoxyglucose uptake was not increased, there was a modest but significantly greater suppression of NEFA after insulin stimulation, which suggests an improved adipocyte insulin response (Table 1) [41]. Additionally, plasma adiponectin levels were modestly increased with *Trib3* ASO. Adiponectin has been reported to improve muscle insulin sensitivity via an AMPK-mediated mechanism [42]. However, in the present study, there were no significant increases in skeletal muscle AMPK activity.

To determine whether the increases in adiposity and improvements in insulin action were due to activation of PPAR-γ, we treated a separate cohort of *Trib3* ASO-treated rats with the PPAR-γ antagonist BADGE. BADGE is a PPAR-γ ligand that antagonises PPAR-γ activation without affecting PPAR-α or PPAR-δ activation [43]. The combination of *Trib3* ASO and BADGE prevented the expansion of fat mass, the increased production of PPAR-γ and its target genes, acyl-CoA oxidase, *Cd36* and *Cebpa*, and the increase in plasma adiponectin. Importantly, BADGE also prevented the improvements in insulin sensitivity with *Trib3* ASO treatment. These results are reminiscent of studies examining the role of forkhead box O1 (FOXO1) in regulation of PPAR-γ production and activation in adipocytes

[19, 44]. These data suggest that the improvements in insulin action observed with *Trib3* knockdown are largely attributable to activation of PPAR-γ.

In addition to the changes in insulin sensitivity, we also found that *Trib3* ASO treatment increased plasma HDL-cholesterol concentration. This was not affected by BADGE co-treatment, suggesting that it was independent of the activation of PPAR-γ. The mechanism for this increase is unclear. We excluded altered levels of *Sr-b1* and *Abca1* as explanations for the increase in HDL. It is possible that *Trib3* ASO leads to increased reverse cholesterol transport though additional studies are required to confirm this. Nonetheless, these favourable changes in lipids persisted with BADGE co-treatment, suggesting that TRIB3 regulates HDL in a manner independent of PPAR-γ.

In summary, these studies provide novel insights into the physiological role of TRIB3 in vivo and its potential as a therapeutic target. Knockdown of *Trib3* clearly improved insulin-stimulated peripheral glucose disposal in insulin-resistant rats. However, contrary to prior studies, these improvements occurred without increased activation of AKT2. Instead, these improvements in insulin sensitivity are largely attributable to activation of PPAR-γ with resultant changes in adipogenesis. Additionally, *Trib3* ASO increased plasma HDL-cholesterol, independenly of PPAR-γ activation. The improvements in insulin action and lipid profile suggest that TRIB3 may be a potential therapeutic target for treating not only the insulin resistance, but also the dyslipidaemia associated with type 2 diabetes mellitus.

Supplementary Material

Refer to Web version on PubMed Central for supplementary material.

Acknowledgments

We thank J. Dong for expert technical assistance with the studies. We also thank A. Groszmann for performing the hormone assays. This work was supported by grants from the US Public Health Service (R01 DK-40936 and P30 DK-45735 to G. I. Shulman) and from the Deutsche Forschungsgemeinschaft (DFG WE 4293/1-1 to D. Weismann).

Abbreviations

AKT	Thymoma viral proto-oncogene
AMPK	AMP-activated protein kinase
ASO	Antisense oligonucleotide
BADGE	Bisphenol-A-diglycidyl ether
FPLC	Fast protein liquid chromatography
PPAR	Peroxisome proliferator-activated receptor
TBST	TBS plus Tween
TRIB	Drosophila tribbles homologue

References

1. Shulman GI. Cellular mechanisms of insulin resistance. J Clin Invest. 2000; 106:171–176. [PubMed: 10903330]
2. Okada T, Kawano Y, Sakakibara T, Hazeki O, Ui M. Essential role of phosphatidylinositol 3-kinase in insulin-induced glucose transport and antilipolysis in rat adipocytes. Studies with a selective inhibitor wortmannin. J Biol Chem. 1994; 269:3568–3573. [PubMed: 8106400]
3. Taniguchi CM, Emanuelli B, Kahn CR. Critical nodes in signalling pathways: insights into insulin action. Nat Rev Mol Cell Biol. 2006; 7:85–96. [PubMed: 16493415]
4. Samuel VT, Liu ZX, Wang A, et al. Inhibition of protein kinase Cepsilon prevents hepatic insulin resistance in nonalcoholic fatty liver disease. J Clin Invest. 2007; 117:739–745. [PubMed: 17318260]
5. Morino K, Petersen KF, Shulman GI. Molecular mechanisms of insulin resistance in humans and their potential links with mitochondrial dysfunction. Diabetes. 2006; 55(Suppl 2):S9–S15. [PubMed: 17130651]
6. Du K, Herzig S, Kulkarni RN, Montminy M. TRB3: a tribbles homolog that inhibits Akt/PKB activation by insulin in liver. Science. 2003; 300:1574–1577. [PubMed: 12791994]
7. Matsushima R, Harada N, Webster NJ, Tsutsumi YM, Nakaya Y. Effect of TRB3 on insulin and nutrient-stimulated hepatic p70 S6 kinase activity. J Biol Chem. 2006; 281:29719–29729. [PubMed: 16887816]
8. Bi XP, Tan HW, Xing SS, et al. Overexpression of TRB3 gene in adipose tissue of rats with high fructose-induced metabolic syndrome. Endocr J. 2008; 55:747–752. [PubMed: 18497449]
9. He L, Simmen FA, Mehendale HM, Ronis MJ, Badger TM. Chronic ethanol intake impairs insulin signaling in rats by disrupting Akt association with the cell membrane. Role of TRB3 in inhibition of Akt/protein kinase B activation. J Biol Chem. 2006; 281:11126–11134. [PubMed: 16452480]
10. Ding J, Kato S, Du K. PI3K activates negative and positive signals to regulate TRB3 expression in hepatic cells. Exp Cell Res. 2008; 314:1566–1574. [PubMed: 18316073]
11. Liu J, Wu X, Franklin JL, et al. Mammalian Tribbles homolog 3 impairs insulin action in skeletal muscle: role in glucose-induced insulin resistance. Am J Physiol Endocrinol Metab. 2010; 298:E565–E576. [PubMed: 19996382]
12. Prudente S, Hribal ML, Flex E, et al. The functional Q84R polymorphism of mammalian Tribbles homolog TRB3 is associated with insulin resistance and related cardiovascular risk in Caucasians from Italy. Diabetes. 2005; 54:2807–2811. [PubMed: 16123373]
13. Shi Z, Liu J, Guo Q, et al. Association of TRB3 gene Q84R polymorphism with type 2 diabetes mellitus in Chinese population. Endocrine. 2009; 35:414–419. [PubMed: 19291425]
14. Prudente S, Scarpelli D, Chandalia M, et al. The TRIB3 Q84R polymorphism and risk of early-onset type 2 diabetes. J Clin Endocrinol Metab. 2009; 94:190–196. [PubMed: 18984671]
15. Andreozzi F, Formoso G, Prudente S, et al. TRIB3 R84 variant is associated with impaired insulin-mediated nitric oxide production in human endothelial cells. Arterioscler Thromb Vasc Biol. 2008; 28:1355–1360. [PubMed: 18436806]
16. Iynedjian PB. Lack of evidence for a role of TRB3/NIPK as an inhibitor of PKB-mediated insulin signalling in primary hepatocytes. Biochem J. 2005; 386:113–118. [PubMed: 15469416]
17. Okamoto H, Latres E, Liu R, et al. Genetic deletion of Trb3, the mammalian Drosophila tribbles homolog, displays normal hepatic insulin signaling and glucose homeostasis. Diabetes. 2007; 56:1350–1356. [PubMed: 17303803]
18. Liew CW, Bochenski J, Kawamori D, et al. The pseudokinase tribbles homolog 3 interacts with ATF4 to negatively regulate insulin exocytosis in human and mouse $\hat{I}^2$ cells. The Journal of Clinical Investigation. 2010; 120:2876–2888. [PubMed: 20592469]
19. Takahashi Y, Ohoka N, Hayashi H, Sato R. TRB3 suppresses adipocyte differentiation by negatively regulating PPARgamma transcriptional activity. J Lipid Res. 2008; 49:880–892. [PubMed: 18187772]
20. Samuel VT, Beddow SA, Iwasaki T, et al. Fasting hyperglycemia is not associated with increased expression of PEPCK or G6Pc in patients with type 2 diabetes. Proc Natl Acad Sci U S A. 2009; 106:12121–12126. [PubMed: 19587243]

21. Erion DM, Ignatova ID, Yonemitsu S, et al. Prevention of hepatic steatosis and hepatic insulin resistance by knockdown of cAMP response element-binding protein. Cell Metab. 2009; 10:499–506. [PubMed: 19945407]
22. Watts LM, Manchem VP, Leedom TA, et al. Reduction of hepatic and adipose tissue glucocorticoid receptor expression with antisense oligonucleotides improves hyperglycemia and hyperlipidemia in diabetic rodents without causing systemic glucocorticoid antagonism. Diabetes. 2005; 54:1846–1853. [PubMed: 15919808]
23. Graham MJ, Crooke ST, Monteith DK, et al. In vivo distribution and metabolism of a phosphorothioate oligonucleotide within rat liver after intravenous administration. J Pharmacol Exp Ther. 1998; 286:447–458. [PubMed: 9655890]
24. Neschen S, Morino K, Rossbacher JC, et al. Fish oil regulates adiponectin secretion by a peroxisome proliferator-activated receptor-gamma-dependent mechanism in mice. Diabetes. 2006; 55:924–928. [PubMed: 16567512]
25. Savage DB, Choi CS, Samuel VT, et al. Reversal of diet-induced hepatic steatosis and hepatic insulin resistance by antisense oligonucleotide inhibitors of acetyl-CoA carboxylases 1 and 2. J Clin Invest. 2006; 116:817–824. [PubMed: 16485039]
26. Hundal RS, Petersen KF, Mayerson AB, et al. Mechanism by which high-dose aspirin improves glucose metabolism in type 2 diabetes. J Clin Invest. 2002; 109:1321–1326. [PubMed: 12021247]
27. Bligh EG, Dyer WJ. A rapid method of total lipid extraction and purification. Can J Biochem Physiol. 1959; 37:911–917. [PubMed: 13671378]
28. Neschen S, Moore I, Regittnig W, et al. Contrasting effects of fish oil and safflower oil on hepatic peroxisomal and tissue lipid content. Am J Physiol Endocrinol Metab. 2002; 282:E395–E401. [PubMed: 11788372]
29. McKay RA, Miraglia LJ, Cummins LL, Owens SR, Sasmor H, Dean NM. Characterization of a potent and specific class of antisense oligonucleotide inhibitor of human protein kinase C-alpha expression. J Biol Chem. 1999; 274:1715–1722. [PubMed: 9880552]
30. Pfaffl MW. A new mathematical model for relative quantification in real-time RT-PCR. Nucleic Acids Res. 2001; 29:e45. [PubMed: 11328886]
31. R Development Core Team. R Foundation for Statistical Computing. Vienna, Austria: ISBN 3-900051-07-0; 2005. R: A language and environment for statistical computing. Available from www.R-project.org.
32. Du K, Ding J. Insulin regulates TRB3 and other stress-responsive gene expression through induction of C/EBPbeta. Mol Endocrinol. 2009; 23:475–485. [PubMed: 19164449]
33. Civitarese AE, Ukropcova B, Carling S, et al. Role of adiponectin in human skeletal muscle bioenergetics. Cell metabolism. 2006; 4:75–87. [PubMed: 16814734]
34. Cheng KK, Iglesias MA, Lam KS, et al. APPL1 potentiates insulin-mediated inhibition of hepatic glucose production and alleviates diabetes via Akt activation in mice. Cell Metab. 2009; 9:417–427. [PubMed: 19416712]
35. Kato S, Du K. TRB3 modulates C2C12 differentiation by interfering with Akt activation. Biochem Biophys Res Commun. 2007; 353:933–938. [PubMed: 17207467]
36. Chen R, Kim O, Yang J, et al. Regulation of Akt/PKB activation by tyrosine phosphorylation. J Biol Chem. 2001; 276:31858–31862. [PubMed: 11445557]
37. Rosen ED. The transcriptional basis of adipocyte development. Prostaglandins, Leukotrienes and Essential Fatty Acids. 2005; 73:31–34.
38. Lefterova MI, Zhang Y, Steger DJ, et al. PPARÎ[3] and C/EBP factors orchestrate adipocyte biology via adjacent binding on a genome-wide scale. Genes & Development. 2008; 22:2941–2952. [PubMed: 18981473]
39. Bezy O, Vernochet C, Gesta S, Farmer SR, Kahn CR. TRB3 blocks adipocyte differentiation through the inhibition of C/EBPbeta transcriptional activity. Mol Cell Biol. 2007; 27:6818–6831. [PubMed: 17646392]
40. Tontonoz P, Spiegelman BM. Fat and beyond: the diverse biology of PPARgamma. Annu Rev Biochem. 2008; 77:289–312. [PubMed: 18518822]

41. Bajaj M, Suraamornkul S, Romanelli A, et al. Effect of a sustained reduction in plasma free fatty acid concentration on intramuscular long-chain fatty Acyl-CoAs and insulin action in type 2 diabetic patients. Diabetes. 2005; 54:3148–3153. [PubMed: 16249438]

42. Bergeron R, Russell RR 3rd, Young LH, et al. Effect of AMPK activation on muscle glucose metabolism in conscious rats. Am J Physiol. 1999; 276:E938–E944. [PubMed: 10329989]

43. Wright HM, Clish CB, Mikami T, et al. A Synthetic Antagonist for the peroxisome proliferator-activated receptor γ Inhibits Adipocyte Differentiation. Journal of Biological Chemistry. 2000; 275:1873–1877. [PubMed: 10636887]

44. Fan W, Imamura T, Sonoda N, et al. FOXO1 transrepresses peroxisome proliferator-activated receptor gamma transactivation, coordinating an insulin-induced feed-forward response in adipocytes. J Biol Chem. 2009; 284:12188–12197. [PubMed: 19246449]

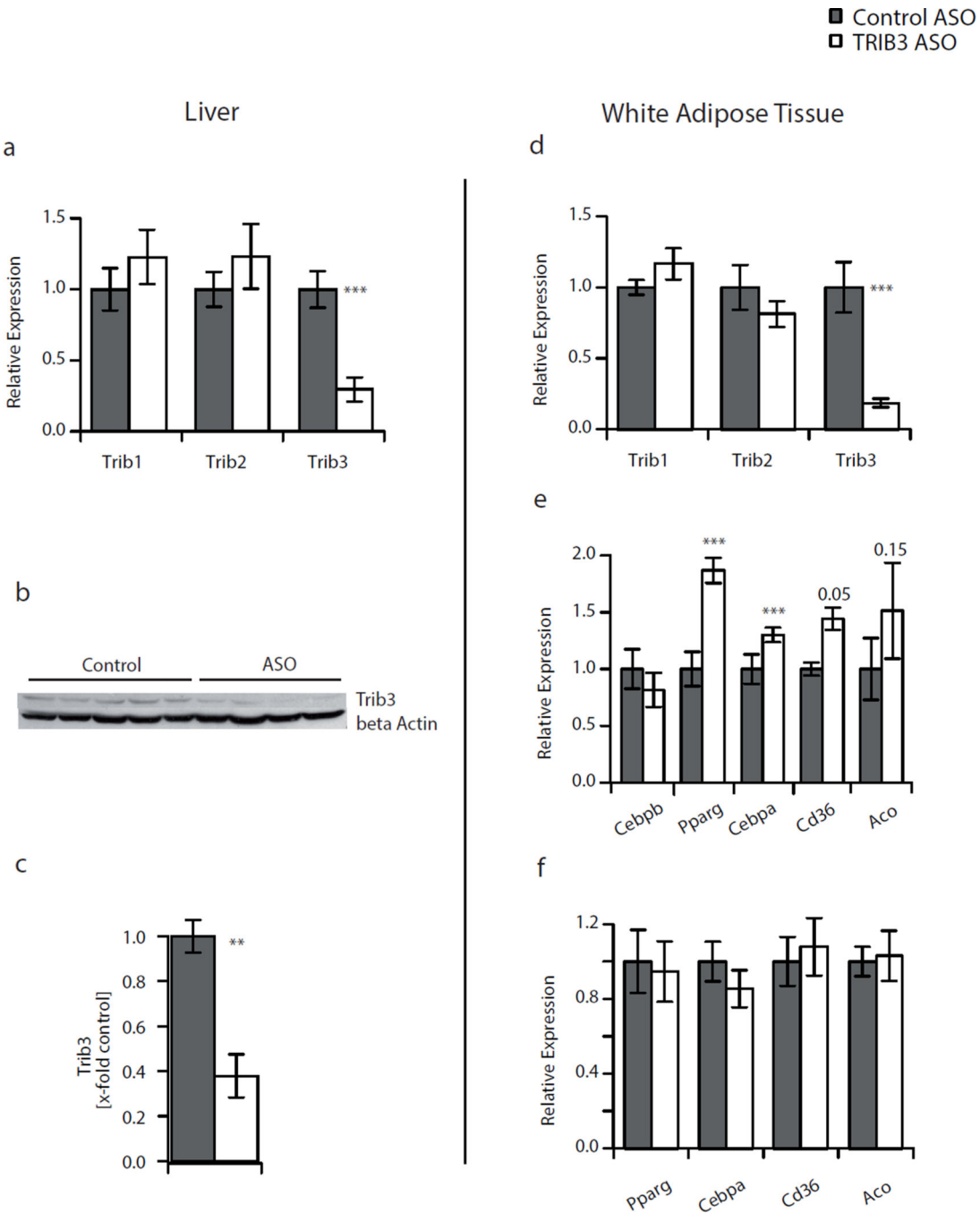

Fig. 1.

Trib3 knockdown and interaction with PPAR-γ. Expression of *Trib1*, *-2* and *-3* after *-4* weeks of *Trib3* ASO treatment (white bars; control ASO, grey bars) in liver (**a**) and white adipose tissue (**d**). TRIB3 protein levels in liver (**b, c**), and (**e**) expression of PPAR-γ, CEBP-B and PPAR-γ-regulated genes in white adipose tissue. **f** Effect of additional BADGE administration after *Trib3* ASO treatment on *Ppar-*γ and PPAR-γ-regulated genes in white adipose tissue. Values are given as mean±SE. $^{**}p<0.01$ and $^{***}p<0.001$, $^{\dagger}p=0.15$, $^{\ddagger}p=0.05$

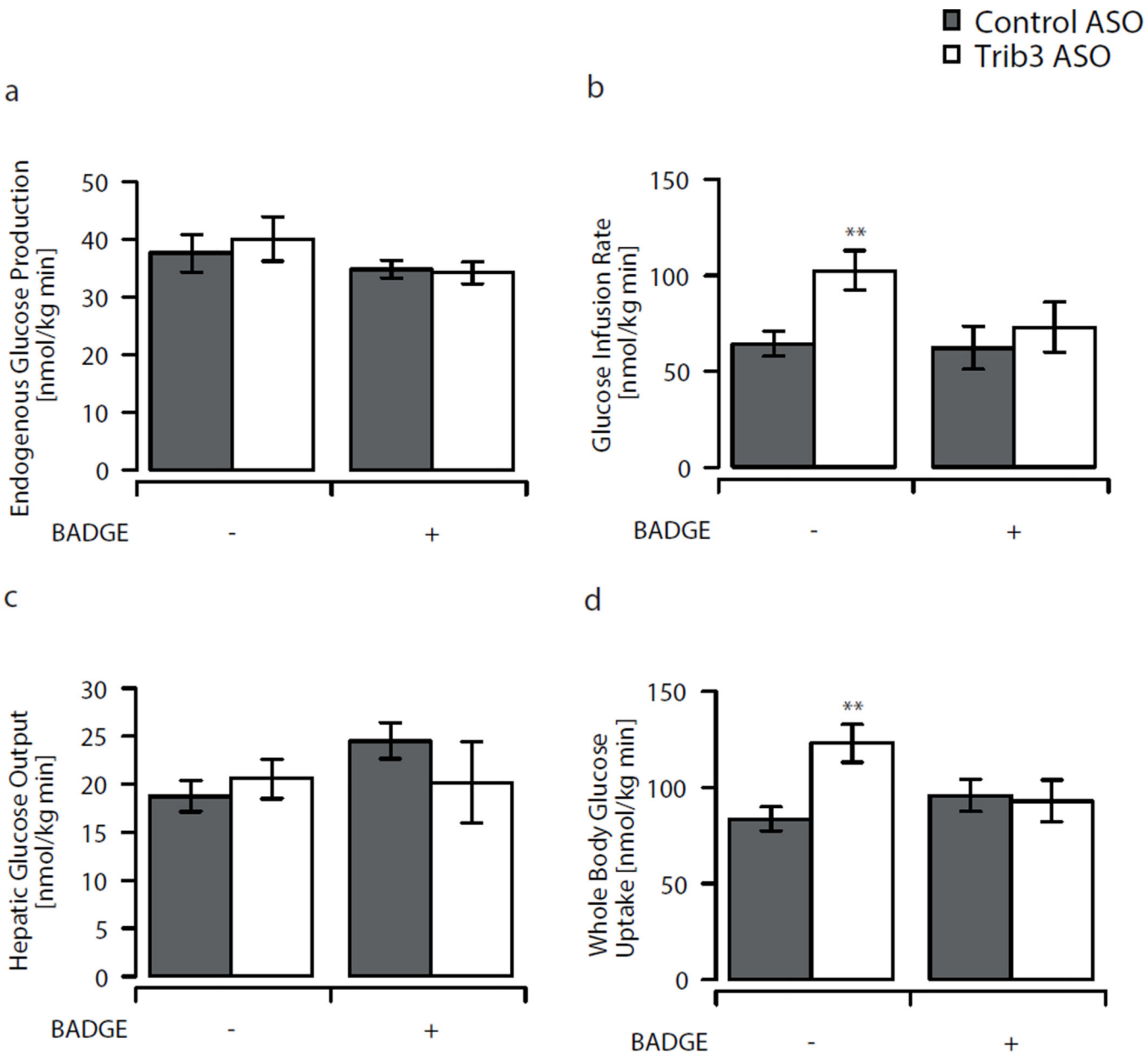

Fig. 2.

Glucose turnover assessed by euglycaemic–hyperinsulinaemic clamps. **a** Endogenous glucose production, (**b**) glucose infusion rate, (**c**) insulin-stimulated hepatic glucose output and (**d**) whole-body glucose turnover in *Trib3* ASO treated (white bars; control ASO, grey bars) animals with and without additional BADGE treatment. Values are given as mean±SE, n=12 per group, n=6–8 per group for BADGE treated animals. **p<0.01

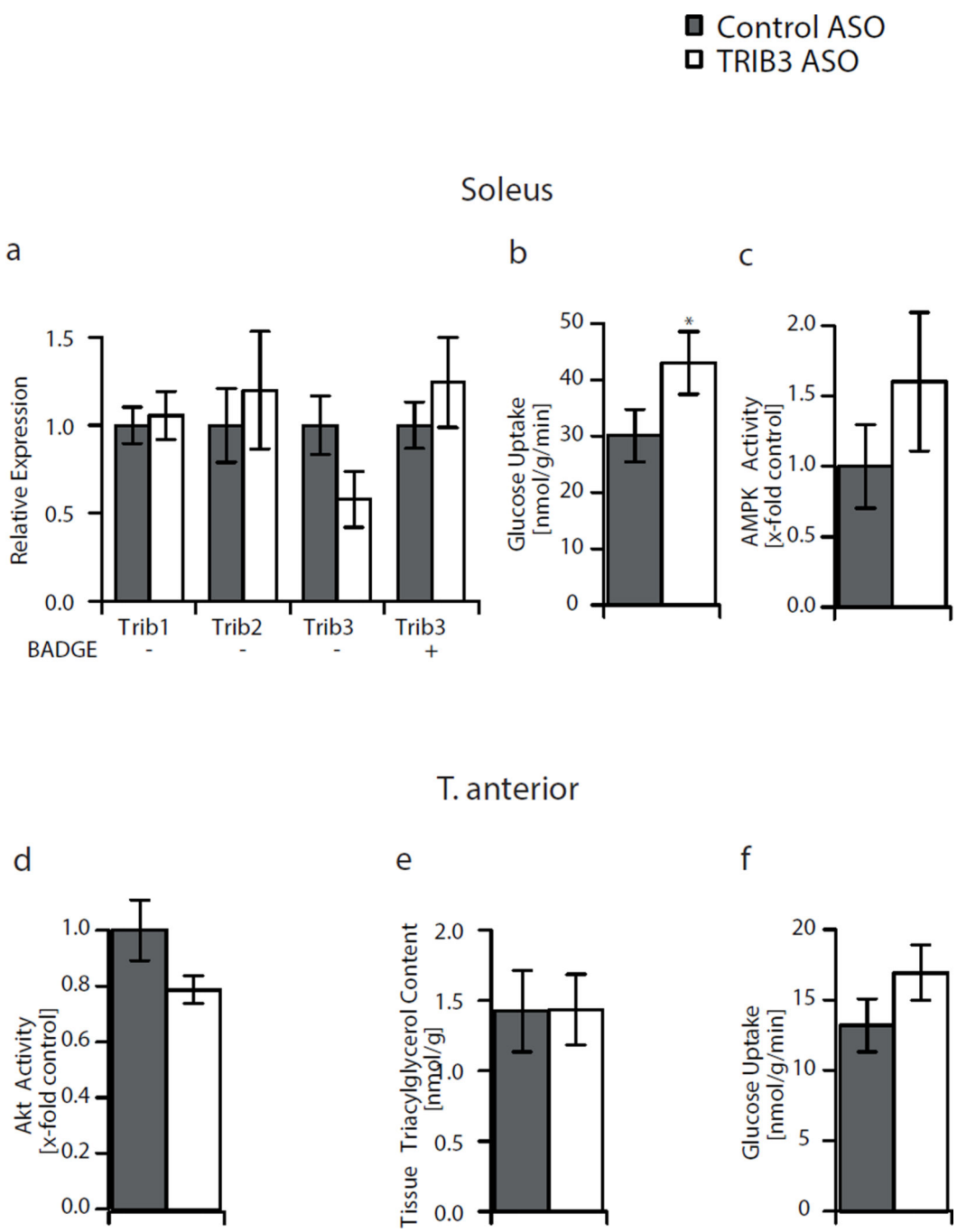

Fig. 3.

Glucose uptake and *Trib3* expression in muscle. **a** Expression of *Trib1, 2, 3* and *Trib3* with BADGE in soleus muscle. **b** Glucose uptake and (**c**) AMPK activity in soleus muscle. **d** AKT2 activity, (**e**) triacylglycerol content and (**f**) glucose uptake in T. anterior. Values are given as mean±SE, *n*=8 per group. **p*<0.05. White bars, TRIB3 ASO; grey bars, control ASO (*Lxra* also known as *Nr1h3*)

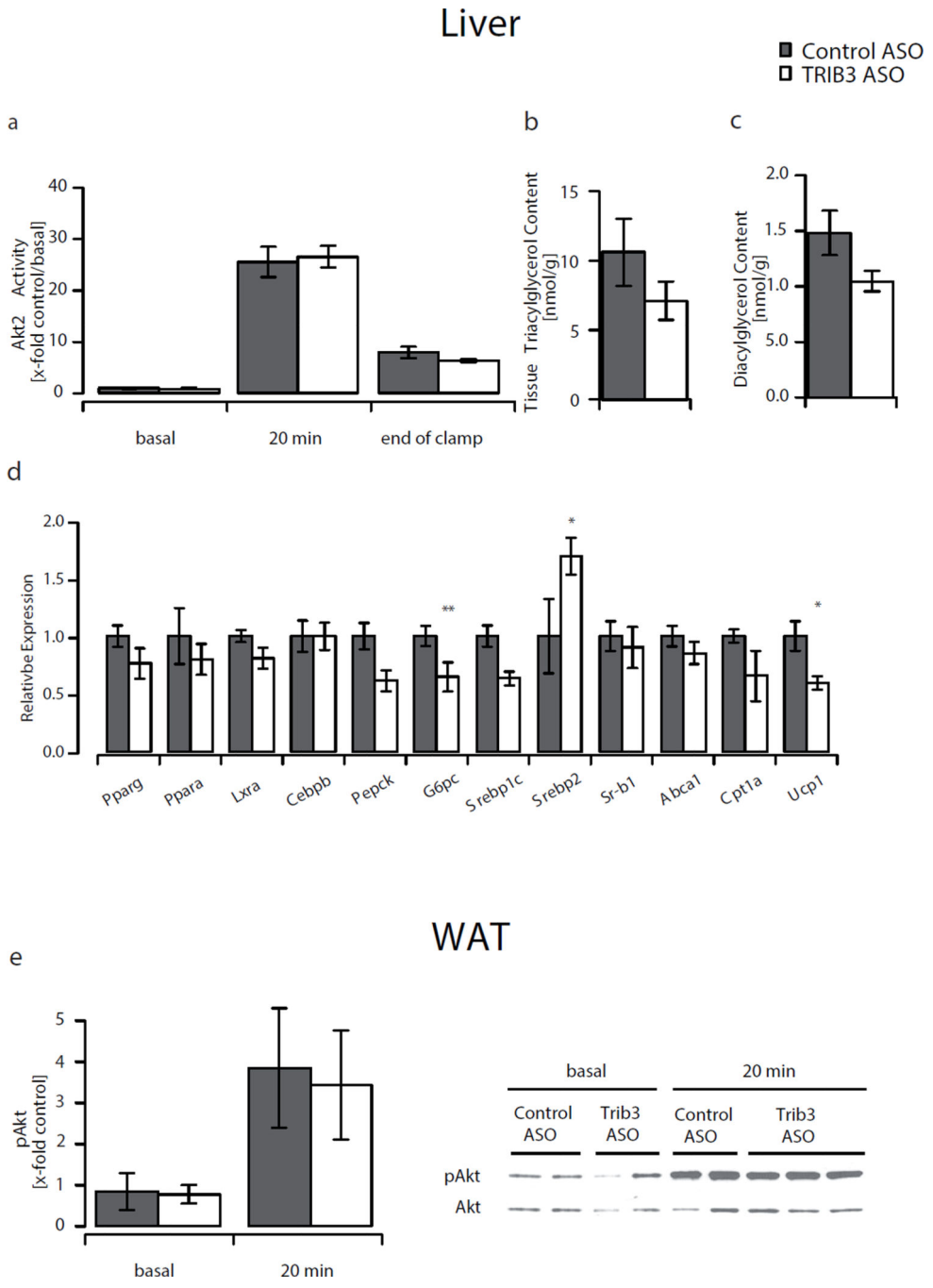

Fig. 4.

Insulin signalling and gene expression in liver. **a** AKT2 activity in liver tissue at times indicated. **b** Liver triacylglycerol and (**c**) diacylglycerol content. **d** Expression of genes important for energy homeostasis, glucose and lipid metabolism in liver. **e** Phosphorylation of AKT in basal white adipose tissue and after 20 min insulin stimulation. Values are given as mean±SE, *n*=7–9 per group. **p*<0.05, ***p*<0.01. White bars, *Trib3* ASO; grey bars, control ASO

Table 1

Biochemical and morphometric data

	Treatment alone			BADGE co-treatment		
Variable	**Control ASO**	***Trib3* ASO**	**Significance**	**Control ASO**	***Trib3* ASO**	**Significance**
Body weight (g)	357.9±8	349.4±6		361.4±6	355±12	
White adipose tissue (g)	3.0±0.2	5.2±0.4	**	4.0±0.3	4.0±0.4	
Leptin (μg/l)	1.6±0.2	2.7±0.6		1.8±0.4	1.9±0.3	
Adiponectin (mg/l)	2.4±0.2	2.9±0.1	*	2±0.3	2.4±0.8	
IL-6 (ng/l)	35.9±9	23.3±9		161±56	260±63	
TNF α (ng/l)	2.9±0.6	2.7±0.3		7.7±2	16±5	
Insulin (pmol/l)	111±28	118±35		250±21	118±21	***
Glucagon (ng/l)	47.6±3	53±6		ND	ND	
Glucose (mmol/l)	6.9±0.1	7.4±0.3		5.7±0.2	5.9±0.2	
ALT (U/l)	44±6	57±9		ND	ND	
AST (U/l)	146±28	192±33		ND	ND	
Cholesterol (mmol/l)	1.5±0.1	2.13±0.2	*	1.5±0.1	2±0.2	
HDL (mmol/l)	0.6±0.05	0.9±0.1	*	0.5±0.05	0.7±0.05	0.05
NEFA (mEq/l)	0.7±0.04	0.8±0.07		0.45±0.07	0.4±0.05	
NEFA suppression (mEq/l)	−0.45±0.05	−0.69±0.06	*	ND	ND	
Plasma triacylglycerol (mmol/l)	0.28±0.03	0.31±0.02		0.6±0.03	0.6±0.7	

Data are presented as mean±SEM

* $p<0.05$,

** $p<0.01$ and

*** $p<0.001$ compared with control ASO

ALT, alanine transferase; AST, aspartate transferase; mEq, milliequivalent; ND, not determined